Volume 13 Number 1
Journal of Advances in Physics

SCINTILLATION EFFECTS AND THE SPATIAL POWER SPECTRUM OF SCATTERED RADIO WAVES IN THE IONOSPHERIC F REGION

[1]George Jandieri, [2]Natalia Zhukova, [3]Zhuzhuna Diasamidze, [4]Mzia Diasamidze
1. Georgian Technical University, 77 Kostava Str., Tbilisi 0175, Georgia
E-mail: jandieri@access.sanet.ge
2. M. Nodia Institute of Geophysics, 1 Aleksidze Str., Tbilisi 0193, Georgia
E-mail: natalia27cpp@hotmail.com
3. Batumi Shota Rustaveli State University, 35 Ninoshvili Str., 6010 Batumi, Georgia
E-mail: zhuzhuna.diasamidze@gmail.com
4. Batumi State Maritime Academy, 53 Rustaveli Av., 6010 Batumi, Georgia
E-mail: mzia.diasamidze@gmail.com

ABSTRACT

Differential equation for two-dimensional spectral function of the phase fluctuation is derived using the modify smooth perturbation method. Second order statistical moments of the phase fluctuations are calculated taking into account polarization coefficients of both ordinary and extraordinary waves in the turbulent collision magnetized plasma and the diffraction effects. Analytical and numerical investigations in the ionospheric F region are based on the anisotropic Gaussian and power law spectral functions of electron density fluctuations including both the field-aligned anisotropy and field-perpendicular anisotropy of the plasma irregularities. Scintillation effects in this region are investigated for the small-scale ionospheric irregularities. The large-scale background plasma structures are responsible for the double-humped shape in the spatial power spectrum taking into account diffraction effects. Numerical calculations are based on the experimental data of the navigation satellites.

Keywords

Scintillation, ionosphere, irregularities, spatial power spectrum, turbulence.

Academic Discipline And Sub-Disciplines

Physics, Plasma physics, Radio physics.

SUBJECT CLASSIFICATION

Electromagnetic theory, Radio waves (theory), Plasma physics

TYPE (METHOD/APPROACH)

Modify smooth perturbation method

INTRODUCTION

At the present time the features of light propagation in random media have been rather well studied [1]. Many articles and reviews are related to the statistical characteristics of scattered radiation and observations in the ionosphere [2-5]. The analysis of the statistical properties of small-amplitude electromagnetic waves that have passed through a plane turbulent plasma slab is very important in many practical applications associated with both natural and laboratory plasmas [6].

Radio signals from communication satellites experience the scintillation phenomenon when received on the ground. The scintillation is caused by the electron density irregularities in the ionosphere. Diffraction effects are importand for small scale plasma irregularities. Interference between propagated radio wave and scattered radiation in the magnetized turbulent ionospheric plasma lead to the scintillation effects at the observation points.

Investigation of statistical characteristics of scattered electromagnetic waves in the ionosphere is of great practical importance. Measurements of the statistical characteristics of scattered electromagnetic waves by satellite, ground-based radar systems or meteorological-ionospheric stations gives the information about ionospheric plasma irregularities. Statistical characteristics of the spatial power spectrum (SPS) (broadening and displacement of its maximum) in the collision magnetized plasma was considered in [7,8] applying the complex geometrical optics approximation and the smooth perturbation methods. Scintillation effects of scattered ordinary and extraordinary waves in the ionospheric plasma for both power-law and anisotropic Gaussian correlation functions of electron density fluctuations have been investigated in [9]. The “Double-Humped Effect” for both above mentioned spectra was investigated analytically and numerically in [9-11] using the modify smooth perturbation method.

The problem is formulated in section 2, where equation for the two-dimensional spectral function of the phase fluctuation is derived and second order statistical moments are presented for arbitrary correlation function of electron density fluctuations. In section 3 analytical and numerical results are presented based on experimental data. Peculiarities

of the scintillation and the SPS are discussed for the ionospheric F-region using both the anisotropic Gaussian and the power low spectral functions characterizing ionospheric plasma irregularities. Some conclusions are made in section 4.

THEORETICAL CONSIDERATIONS

The electric field in the magnetized ionospheric plasma with anisotropic electron density irregularities satisfies the wave equation:

$$\left(\frac{\partial^2}{\partial x_i \, \partial x_j} - \Delta \delta_{ij} - k_0^2 \, \varepsilon_{ij}(\mathbf{r}) \right) \mathbf{E_j}(\mathbf{r}) = 0 \, . \tag{1}$$

with the components of the second order permittivity tensor [12]:

$$\varepsilon_{xx} = 1 - \frac{\mathrm{v}\, g}{g^2 - u} \, , \quad \varepsilon_{xy} = -\, \varepsilon_{yx} = i \, \frac{\mathrm{v}\sqrt{u}\cos\alpha}{g^2 - u} \, , \quad \varepsilon_{xz} = -\, \varepsilon_{zx} = -\, i \, \frac{\mathrm{v}\sqrt{u}\, \sin\alpha}{g^2 - u} \, ,$$

$$\varepsilon_{yy} = 1 - \frac{\mathrm{v}(g^2 - u\, \sin^2\alpha)}{g\,(g^2 - u)} \, , \quad \varepsilon_{yz} = \varepsilon_{zy} = \frac{u\, \mathrm{v} \sin\alpha \cos\alpha}{g\,(g^2 - u)} \, , \quad \varepsilon_{zz} = 1 - \frac{\mathrm{v}(g^2 - u\, \cos^2\alpha)}{g\,(g^2 - u)} \, , \tag{2}$$

where: $g = 1 - i\, s$, $s = \nu_{eff} / \omega$, $\nu_{eff} = \nu_{ei} + \nu_{en}$ is the effective collision frequency of electrons with other plasma particles, α is the angle between the *Z*-axis (the direction of radio wave propagation) and the external magnetic field $\mathbf{H_0}$ in the *YOZ* principle plane; $\omega_p(\mathbf{r}) = [4\pi N(\mathbf{r}) e^2 / m]^{1/2}$ is the plasma frequency, $N(\mathbf{r})$ is the electron density, e and m are the charge and mass of electrons respectively, $u(\mathbf{r}) = (e\, H_0(\mathbf{r}) / m\, c\, \omega)^2$ and $\mathrm{v}(\mathbf{r}) = \omega_p^2(\mathbf{r}) / \omega^2$ are the magneto-ionic parameters, Δ is the Laplacian, $\delta_{i\,j}$ is the Kronecker symbol. The dielectric permittivity of the turbulent magnetized plasma is a random function of the spatial coordinates: $\varepsilon_{ij}(\mathbf{r}) = \varepsilon_{ij}^{(0)} + \varepsilon_{ij}^{(1)}(\mathbf{r})$, $|\, \varepsilon_{ij}^{(1)}(\mathbf{r}) | << 1$. First term is a regular (unperturbed) component; the second one describes turbulence: $\mathrm{v}(\mathbf{r}) = \mathrm{v}_0\, [1 + n_1(\mathbf{r})]$. Scintillations are caused due to electron density fluctuations. At high frequency the effect of ions can be neglected. The geomagnetic field leads to the birefringence and anisotropy of scattered electromagnetic waves.

Polarization coefficients in the collision magnetized plasma are [11] expressed via magneto-ionospheric parameters:

$$\frac{< E_y >_{1,2}}{< E_x >_{1,2}} = -\, i\, \mathrm{P}''_j - s\, \mathrm{P}'_j \, , \qquad \frac{< E_z >_{1,2}}{< E_x >_{1,2}} = i\, \Gamma''_j + s\, \Gamma'_j \, , \tag{3}$$

where: $\mathrm{P}''_j = \dfrac{2\sqrt{u_L}}{u_T \mp \sqrt{a_0}} \left[(1 - \mathrm{v}) \mp 2 s^2 \dfrac{u_L (5 - 4\,\mathrm{v})}{\sqrt{a_0}\,(u_T \mp \sqrt{a_0})} \right] = \mathrm{P}''_1 \mp s^2\, \mathrm{P}''_2$, $\quad u_T = u\, \sin^2\alpha$, $\quad u_L = u\, \cos^2\alpha$,

$$\mathrm{P}'_j = \frac{2\sqrt{u_L}}{u_T \mp \sqrt{a_0}} (1 \pm D) + 2 s^2 \, \frac{u_L}{\sqrt{a_0}\,(u_T \mp \sqrt{a_0})} \left[\pm \frac{D\,(u_T \mp 2\sqrt{a_0})}{\sqrt{a_0}} \mp (1 \pm D) \right] = \mathrm{P}'_1 + s^2\, \mathrm{P}'_2 \, ,$$

$$a_0 = u_T^2 + 4 u_L (1 - \mathrm{v})^2 \, , \qquad D = \frac{4 u_L (1 - \mathrm{v})^2}{\sqrt{a_0}\,(u_T \mp \sqrt{a_0})} \, , \qquad \tau_0 = 1 - u - \mathrm{v} + \mathrm{v}\, u_L \, , \qquad \tau_1 = 3 + u - 2\,\mathrm{v} \, ,$$

$$\Gamma'_j = \frac{\sqrt{u_T}}{\tau_0^2} \left[\mathrm{v}\,(\tau_0 + \tau_1) + \sqrt{u_L}\,(\tau_1\, \mathrm{P}''_1 + \tau_0\, \mathrm{P}'_1) + s^2 \sqrt{u_L}\,(\mp \tau_1\, \mathrm{P}''_2 + \tau_0\, \mathrm{P}'_2) \right] = \Gamma'_1 + s^2\, \Gamma'_2$$

$$\Gamma''_j = \frac{\sqrt{u_T}}{\tau_0} (\mathrm{v} + \sqrt{u_L}\ \mathrm{P}''_1) - s^2 \, \frac{\sqrt{u_T}}{\tau_0^2} \left\{ \pm \sqrt{u_L}\, \mathrm{P}''_2 + \frac{1}{\tau_0} \left[\mathrm{v}\, \tau_1 + (3 - \mathrm{v}) \sqrt{u_L}\, \mathrm{P}''_1 + \tau_1 \sqrt{u_L}\ \mathrm{P}'_1 \right] \right\} = \Gamma''_1 - s^2\, \Gamma''_2 \, ,$$

upper sign (index 1) corresponds to the ordinary wave; the lower sign (index 2) to the extraordinary wave. If electron concentration in the slab varies in the interval $0 < \mathrm{v} < 1$ there is no reflection area for the ordinary wave propagation; the same condition is fulfilled for the extraordinary wave at $0 < \mathrm{v} < 1 - \sqrt{u}$. Inclusion of an external magnetic field at $u < 1$ increases fluctuations of the extraordinary wave and decreases fluctuations of the ordinary wave. However situation can be changed at $u > 1$. In this case external magnetic field may reduce fluctuation level of both waves.

We introduce the wave field as [10,13]: $E_j(\mathbf{r}) = E_{0j}\exp\{\Phi(\mathbf{r})\}$, where $\Phi(\mathbf{r})$ is the complex phase, which is presented as a sum $\Phi(\mathbf{r}) = \varphi_0 + \varphi_1 + \varphi_2 + \ldots$, $\varphi_0 = ik_0 x + ik_\perp y$ ($k_\perp << k_0$). Complex phase fluctuations are of the order $\varphi_1 \sim \varepsilon_{ij}^{(1)}$, $\varphi_2 \sim \varepsilon_{ij}^{(1)\,2}$, parameter $\mu = k_\perp / k_0$ describes the diffraction effects.

Taking into account inequalities characterizing the smooth perturbation method [1,14] in the first approximation we have [10,11,13]:

$$\left[\frac{\partial^2\varphi_1}{\partial x_i\,\partial x_j} + \frac{\partial\varphi_0}{\partial x_i}\frac{\partial\varphi_1}{\partial x_j} + \frac{\partial\varphi_1}{\partial x_i}\frac{\partial\varphi_0}{\partial x_j} - \delta_{ij}\left(\Delta_\perp + 2ik_\perp\frac{\partial\varphi_1}{\partial y} + 2ik_0\frac{\partial\varphi_1}{\partial z}\right) - k_0^2\,\varepsilon_{ij}^{(0)}\right]E_{0j} = 0\ . \tag{4}$$

where $\Delta_\perp = (\partial^2\varphi_1/\partial x^2) + (\partial^2\varphi_1/\partial y^2)$ is the transversal Laplasian.

Fourier transformation for the phase fluctuations is

$$\varphi_1(x,y,z) = \int_{-\infty}^{\infty} d\,k_x \int_{-\infty}^{\infty} d\,k_y\ \psi(k_x,k_y,z)\exp(ik_x x + ik_y y)\,,$$

while the 2D spectral function of the phase fluctuation satisfies the stochastic differential equation:

$$\frac{\partial\psi}{\partial t} + \frac{i\,d_1 - d_2}{\Gamma''k_x + i\,(2k_0 - s\Gamma' k_x)}\,\psi(\mathbf{æ},z) = -\frac{k_0^2}{\Gamma''k_x + i\,(2k_0 - s\Gamma' k_x)}\left[\mathrm{T}_1(\mathbf{æ},z) + i\,s\,\mathrm{T}_2(\mathbf{æ},z)\right], \tag{5}$$

where: $\mathbf{æ} = (k_x,k_y)$ is the wave number vector perpendicular to the Z axis, $d_1 = k_x\left[k_0\,\Gamma_j'' - \mathrm{P}_j''(k_y + k_\perp)\right]$, $d_2 = k_y(k_y + 2k_\perp) + s\,k_x\left[\mathrm{P}_j'(k_y + k_\perp) - \Gamma_j'\,k_0\right]$. Random functions $\mathrm{T}_1(\mathbf{æ},z)$ and $\mathrm{T}_2(\mathbf{æ},z)$ containing components of the permittivity tensors and fluctuating term of electron density fluctuations can be easily reproduced from equations (2).

Phase fluctuations of scattered electromagnetic wave satisfying the boundary condition $\varphi_1(k_x,\,k_y,\,z=0) = 0$ has the following form:

$$\varphi_1(x,y,L) = i\,\frac{k_0}{2}\,(Z' + i\,s\,Z'')\int_{-\infty}^{\infty} dk_x \int_{-\infty}^{\infty} dk_y \int_0^L dz'\,n_1(k_x,k_y,z')\exp(i\,k_x\,x + i\,k_y\,y)\cdot$$

$$\cdot\exp\left(\frac{1}{4k_0^2}\left\{\left[d_2\,\Gamma_j''\,k_x - d_1(2k_0 - s\Gamma_j'\,k_x)\right] - i\left[d_1\,\Gamma_j''\,k_x + d_2(2k_0 - s\Gamma_j'\,k_x)\right]\right\}\cdot(L - z')\right), \tag{6}$$

where: $Z' = -\frac{\mathrm{v}}{1-u}\,(1 + \sqrt{u_L}\,\mathrm{P}_1'' - \sqrt{u_T}\,\Gamma_1'') + s^2\,\frac{\mathrm{v}}{1-u}\left[\sqrt{u_L}\left(\pm\mathrm{P}_2'' - \frac{2}{1-u}\,\mathrm{P}_1'\right) + \sqrt{u_T}\left(-\Gamma_2'' + \frac{2}{1-u}\,\Gamma_1'\right)\right]$,

$$Z'' = -\frac{\mathrm{v}}{1-u}\left[\frac{1+u}{1-u} - \sqrt{u_L}\left(\mathrm{P}_1' - \frac{2}{1-u}\,\mathrm{P}_1''\right) + \sqrt{u_T}\left(\Gamma_1' - \frac{2}{1-u}\,\Gamma_1''\right)\right] +$$

$$+ s^2\,\frac{\mathrm{v}}{1-u}\left[\sqrt{u_L}\left(\mathrm{P}_2' \pm \frac{2}{1-u}\,\mathrm{P}_2''\right) - \sqrt{u_T}\left(\Gamma_2' + \frac{2}{1-u}\,\Gamma_2''\right)\right],$$ L is the path length.

Second order statistical moment $W_\varphi(\mathbf{æ},L)$ is expressed via arbitrary 3D spectral function of the correlation function of electron density fluctuations $V_n(\mathbf{k})$:

$$W_\varphi(\boldsymbol{\rho},L) > \equiv < \varphi_1(\mathbf{r})\,\varphi_1^*(\mathbf{r}+\boldsymbol{\rho}) > = \frac{\pi}{2}\,(Z'^2 + s^2\,Z''^2)\,k_0^2\,L\int_{-\infty}^{\infty} dk_x \int_{-\infty}^{\infty} dk_y\ V_n\left\{k_x,k_y,-\frac{1}{4k_0^2}\left[2\,k_0(2k_\perp + k_y)k_y + \right.\right.$$

$$\left.\left. + \Lambda_0\,k_x^2 - s\Lambda_1\,k_x\right]\cdot\exp(-\,i\,k_x\,\rho_x - i\,k_y\,\rho_y)\right\}, \tag{7}$$

where: $\Lambda_0 = \Lambda_2 - (\Gamma''\mathrm{P}' + s^2\,\Gamma'\mathrm{P}')\,k_y$, $\Lambda_2 = \Gamma''(\Gamma''k_0 - \mathrm{P}''k_\perp) + s^2(\Gamma' k_0 - \mathrm{P}' k_\perp)$,

$\Lambda_1 = 2k_0\,(\Gamma' k_0 - \mathrm{P}' k_\perp) + 2(\Gamma' k_\perp - \mathrm{P}' k_0)\,k_y + \Gamma' k_y^2$, ρ_y and ρ_x are distances between observation points spaced apart in the principle and perpendicular planes, respectively. Phase fluctuations at different observation points are not independent and they correlate. The asterisk indicates the complex conjugate, the angular brackets indicate the statistical average.

The fluctuations in the ionosphere can be characterized by the phase structure function, which is the variance of the phase difference between two probes as a function of their separation [1,6,14] and can be calculated using equation (7):

$$D_1(\mathbf{r_1}, \mathbf{r_2}) = < \left(\varphi_1(\mathbf{r_1}) - \varphi_1(\mathbf{r_2})\right)\left(\varphi_1^*(\mathbf{r_1}) - \varphi_1^*(\mathbf{r_2})\right) > . \tag{8}$$

The angle-of-arrivals (AOA) in the principle and perpendicular planes are [1,14]:

$$< \Theta_x^2 > = \lim_{\eta_x \to 0} \frac{D_1(\eta_x, 0, L)}{\eta_x^2}\ , \qquad < \Theta_y^2 > = \lim_{\eta_y \to 0} \frac{D_1(0, \eta_y, L)}{\eta_y^2}\ . \tag{9}$$

The small fluctuations in the AOA of the received signal can be used to obtain some information about the ionosphere, $\eta_x = k_0\,\rho_x$, $\eta_y = k_0\,\rho_y$ are nondimensional parameter .

The variance of the frequency fluctuations of scattered electromagnetic waves $< \omega_1^2 >$ determines the width of the temporal power spectrum measured by experiments. It depends on the parameters characterizing anisotropic plasma irregularities and the absorption caused by collision of electrons with other plasma particles. Correlation function of the frequency fluctuations is calculated as [15]:

$$W_\Omega(\eta_x, 0, L) \equiv -\ k_0^2\, V_0^2 \left[\frac{\partial^2 W_\varphi(\eta_x, 0, L)}{\partial \eta_x^2} \cos^2\theta + \frac{1}{\eta_x} \frac{\partial W_\varphi(\eta_x, 0, L)}{\partial \eta_x} \sin^2\theta \right], \tag{10}$$

where θ is the angle between the direction of the uniform drift velocity $\mathbf{V_0}$ and vector $\boldsymbol{\eta}$. This velocity of the irregularities assumed to be frozen in a direction transverse to the signal path. In this case $W_\Omega(\eta_x, 0, L)$ function is anisotropic due to the presence of the wind direction even at isotropic correlation function of phase fluctuations. Calculation of the second order moment (10) allows to estimate geometrical parameters of the anisotropic plasma irregularities and the drift velocity with which the plasma irregularities drift across the signal path without changing their characteristics.

The standard relationship for weak scattering between the scintillation level S_4 and the 2D phase spectrum describing 2D diffraction pattern on the ground is [16]:

$$S_4^2 = 2 \int_{-\infty}^{\infty} dk_x \int_{-\infty}^{\infty} dk_y\, W_\varphi(k_x, k_y, L) \sin^2\left(\frac{k_x^2 + k_y^2}{k_f^2} \right), \tag{11}$$

where: $k_f = (4\pi / \lambda z)^{1/2}$ is the Fresnel wavenumber. The double integral in the wave number space not depends on the intensity fluctuations and depends on the shape of the fluctuation spectrum. The sinusoidal term is responsible for oscillations in the scintillation spectrum. The value of the scintillation index depends on geometry, frequency and the ionization irregularity structure. Phase scintillations are usually observed as a phase difference between the antennas of an interferometer system. The spatial autocorrelation function of the diffraction pattern could be measured with a suitable two-dimensional array of sensors.

Transverse correlation function of a scattered field $W_{EE^*}(\boldsymbol{\rho}) = < E(\mathbf{r})\, E^*(\mathbf{r} + \boldsymbol{\rho}) >$ containing variances of the phase fluctuations in the first and second approximations has the following form [17,18]:

$$W_{EE^*}(\boldsymbol{\rho}, k_\perp) = E_0^2\ \exp(-i\,\rho_y\, k_\perp)\ \exp\left[\frac{1}{2} \left(< \varphi_1^2(\mathbf{r}) > + < \varphi_1^{*2}(\mathbf{r} + \boldsymbol{\rho}) > \right) \right] \exp\left(2\,\mathrm{Re} < \varphi_2 >\right) \cdot$$

$$\cdot\ \exp\left[< \varphi_1(\mathbf{r})\ \varphi_1^*(\mathbf{r} + \boldsymbol{\rho}) > \right], \tag{12}$$

where E_0^2 is the intensity of an incident radiation.

SPS of a scattered field in case of an incident plane wave $W(k, k_\perp)$ is easily calculated by Fourier transform of the transversal correlation function of a scattered field [19]:

$$W(k,k_\perp)=\int_{-\infty}^{\infty} d\rho_y\, W_{EE^*}(\rho_y,k_\perp)\exp(i\,k\rho_y)\,. \tag{13}$$

NUMERICAL RESULTS

The incident electromagnetic wave has the frequency of 40 MHz ($k_0=0.84\ \mathrm{m}^{-1}$). Plasma parameters at the altitude of 300 km are: $u=0.0012$, $\mathrm{v}=0.0133$. The first Fresnel's radius and the Fresnel wavenumber are equal to 1.5 km and 2.4 km^{-1}, respectively.

An RH-560 rocket flight was conducted from Sriharikota rocket range (SHAR), India (14^0 N, 80^0 E, dip latitude 5.5^0 N) to study electron density irregularities during spread F. It was found that the irregularities were present continuously between 150 and 257 km. The most intense irregularities occurred in three patches at 165-178 km, 210-257 km and 290-330 km [20,21]. Studing the equatorial spread F irregularities using RH-560 rocket instrumented with Langmuir probes launched from SHAR it was established [20,21] that the relationship between the spectral index, *p* and the mean integrated spectral power (in 20 m to 200 m scale size range) could be represented by a Gaussian function.

The anisotropic 3D Gaussian autocorrelation function describing narrow-band process has the following form [7]:

$$V_n(k_x,k_y,k_z)=\sigma_n^2\,\frac{l_\perp^2\,l_\parallel}{8\pi^{3/2}}\,\exp\left(-\frac{k_x^2\,l_\perp^2}{4}-p_1\frac{k_y^2\,l_\parallel^2}{4}-p_2\frac{k_z^2\,l_\parallel^2}{4}-p_3\,k_y\,k_z\,l_\parallel^2\right), \tag{14}$$

where: $p_1=(\sin^2\gamma_0+\chi^2\cos^2\gamma_0)^{-1}\left[1+(1-\chi^2)^2\sin^2\gamma_0\cos^2\gamma_0/\chi^2\right]$, $p_2=(\sin^2\gamma_0+\chi^2\cos^2\gamma_0)/\chi^2$,

$p_3=(1-\chi^2)\sin\gamma_0\cos\gamma_0/2\chi^2$, σ_n^2 is the mean-square fractional deviation of electron density. Diffusion processes along and across directions with respect to the geomagnetic lines of force leads to the anisotropy of plasma irregularities in the ionospheric F-region. The shape of electron density irregularities has a spheroidal form with its axis along the magnetic field line. Elongated spheroid characterizes by anisotropy coefficient $\chi=l_\parallel/l_\perp$, the ratio of longitudinal and transverse linear sizes of plasma irregularities, and the slope angle γ_0 of its axis to the geomagnetic lines of force. The structure, the generation and the evolution of plasma irregularities are dependent on the condition in the ionospheric F-region.

For small-scale ionospheric irregularities having characteristic linear scale ~1 km the ratio of the diffusion coefficients along and transverse directions with respect to the geomagnetic field on the altitude 300 km is $D_\parallel/D_\perp\sim(\nu_{in}^2+\Omega_i^2)/\nu_{in}^2\sim10^4-10^5$, taking into account that the diffusion coefficients are proportional to the corresponding mobility and the diffusion spread of the ionospheric irregularities are determined by ions mobility, not by electrons mobility. Solving the diffusion equation and taking into account the initial conditions it is easily to show that for creation of elongated ionospheric irregularities along the external magnetic field having anisotropy factor ≥10 it is necessary time ≥2 minutes. We should also to point out that lifetime of ionospheric irregularities is determined by turbulence varying substantially along latitude but not by diffusion.

Measurements of satellite's signal parameters passing through the ionospheric slab and measurements aboard of satellite show that in the ionospheric F-region irregularities have power-law spectrum with different spatial scales and is defined as [7]:

$$W_N(\mathbf{k})=\frac{\sigma_N^2}{2\pi^2}\,\frac{\Gamma\left(\frac{p}{2}\right)\Gamma\left(\frac{5-p}{2}\right)}{\Gamma\left(\frac{3}{2}\right)}\,\sin\left[\frac{(p-3)\pi}{2}\right]\,\frac{l_\perp^2\,l_\parallel}{\left[1+l_\perp^2(k_\perp^2+\chi^2k_\parallel^2)\right]^{p/2}}\ , \tag{15}$$

where $k_\perp$ and $k_\parallel$ indicate the perpendicular to the magnetic field and field aligned wave numbers respectively. In this formula Γ is the gamma function, p is the power index. Although generation mechanisms of irregularities in the magnetized turbulent ionospheric plasma is substantially different, we will use both 3D Gaussian and power law spectra.

We consider both large (characteristic linear scales about ten hundred km) and small scale (dimensions several hundred meters) irregularities. Anisotropy degree of small scale irregularities varies from 1.1 up to 5.5. Slope angle of elongated irregularities with respect to the geomagnetic lines of forces varies in the interval 8^0-28^0. Mean anisotropy factor of large scale irregularities is equal to 2.8, maximum is 6 [22].

An RH-560 rocket flight was conducted to study electron density irregularities during spread F caused due to the gradient drift instability. It was found [21] that the average spectral index of transitional (10-100 m) scale size range for 160-178 km, 210-250 km 250-280 km and 290-330 km regions is – 3.99, – 4.33, – 3.36 and – 3.17, respectively. The irregularities in this scale are presented in plenty in 220-250 km and 290-330 km regions with an average spectral index of – 4.32.The average spectral index of intermediate (100 m-2 km) scale irregularities in 160-170 km was found to be – 3.78; in 220-250 km and 290-320 km regions can be presented by -3.4 ± 0.5 [21].

Substituting equation (14) into (7), we obtain:

$$W_{\varphi}(s,\boldsymbol{\eta})=\frac{\xi\,\Omega_0}{2\sqrt{\pi}\,\chi}\int_{-\infty}^{\infty}dx\int_{-\infty}^{\infty}dy\;\exp\left\{-\frac{\xi^2}{4}\left[\frac{p_2}{16}\Lambda_0'^2\,x^4+\left(\frac{1}{\chi^2}+\Psi_0\,\Lambda_0'\right)x^2+J_1\right]+\right.$$

$$\left.+\frac{\xi^2}{4}\,s\Lambda_1'\left(\frac{p_2}{8}\Lambda_0'\,x^3-\Psi_0\,x\right)-\frac{\xi^2}{4}s^2\left[\frac{p_2}{8}\Lambda_0'\,\Lambda_0''\,x^4+\left(\Psi_0\,\Lambda_0''+\frac{p_2}{16}\,\Lambda_1'^2\right)x^2\right]\right\}\exp(-i\,\eta_x\,x-i\,\eta_y\,y)\,, \qquad (16)$$

where: $\Psi_0=\frac{p_2}{4}\,y^2+\left(\frac{p_2}{2}\,\mu-p_3\right)y$, $\Omega_0=\sigma_n^2\,\frac{\xi^2\,k_0L}{8\chi}\,(Z'^2+s^2Z''^2)$,

$J_1=\frac{p_2}{4}\,y^4+(p_2\,\mu-2p_3)y^3+(p_1+p_2\,\mu^2-4p_3\,\mu)\,y^2$.

This correlation function is valid for all levels of scintillations.

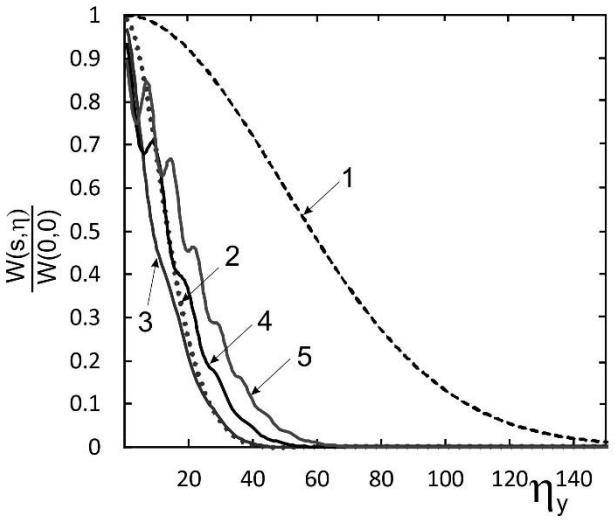

Fig. 1: Correlation function of the phase fluctuations versus distance between observation points in the principle plane. Curve 1 corresponds to the isotropic case $\chi=1$ and $\gamma_0=0^0$; curve 2 depicts anisotropic plasma irregularities with anisotropy factor $\chi=5$, $\gamma_0=5^0$; curve 3: $\chi=10$, $\gamma_0=10^0$; curve 4: $\chi=15$, $\gamma_0=15^0$; curve 5: $\chi=20$, $\gamma_0=20^0$.

Figure 1 shows variation of the anisotropic Gaussian correlation function of the phase fluctuations as a function of distance between observation points in the direction perpendicular to the geomagnetic field. Smooth spectrum corresponds to the isotropic plasma irregularities ($\chi=1$). Numerical calculations show that increasing anisotropy factor of ionospheric plasma irregularities, correlation function for both ordinary and extraordinary waves fast dumping. Oscillations are observed at big anisotropy factors.

Figures 2 and 3 depict wave structure function (8) for the correlation function of the phase fluctuations for the extraordinary wave in the principle and perpendicular planes. Dimensionless collision frequency between plasma particles in the ionospheric F-region is $s=10^{-3}$, characteristic linear scale of plasma irregularities is about 80 meters, diffraction parameter $\mu=0.06$. Numerical calculations are carrying out for the anisotropy factors $\chi=5-17$, inclination angle of elongated plasma irregularities along the external magnetic field varies in the interval $\gamma_0=5^0-20^0$.

For HF wave modes the shapes of the ordinary and extraordinary structure functions are differ in the principle and perpendicular planes. Analyses of the numerical calculations show that that the diffraction effects, anisotropy of plasma irregularities and collision between plasma particles lead to the oscillations (Figure 2) of the phase structure function

$D_1(\mathbf{r_1}, \mathbf{r_2})$ in the principle plane at small distances between observation points $0 \le \eta_y \le 30$ for both waves.

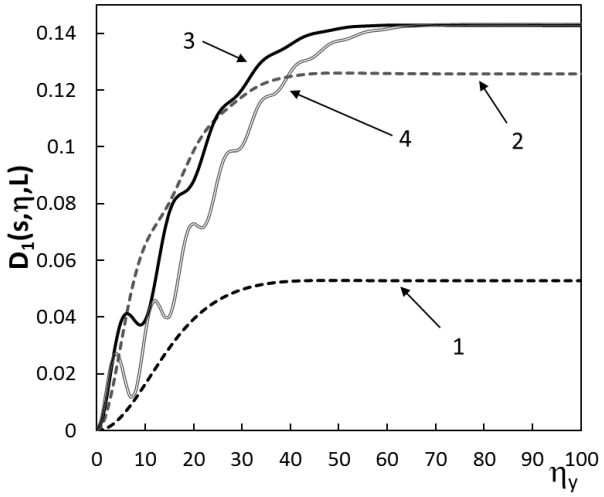

Fig. 2: Plots of phase structure function of the extraordinary wave versus distance between observation points in the principle plane. Curve 1: $\chi = 5$, $\gamma_0 = 5^0$; curve 2: $\chi = 10$, $\gamma_0 = 10^0$; curve 3: $\chi = 15$, $\gamma_0 = 15^0$; curve 4: $\chi = 17$, $\gamma_0 = 20^0$.

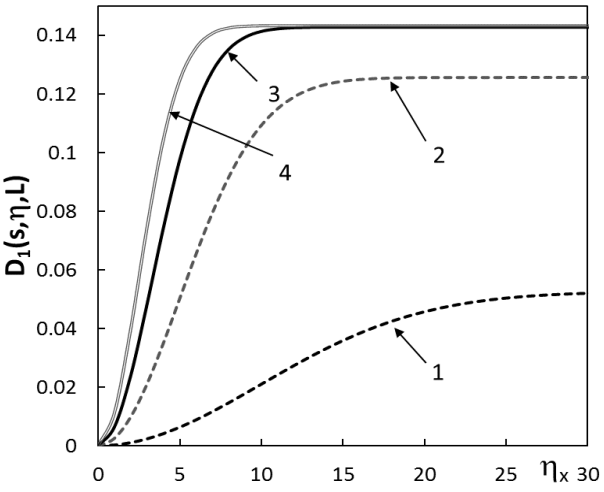

Fig. 3: Plots of phase structure function of the extraordinary wave versus distance between observation points perpendicular to the principle plane. Designations are the same as on Fig. 2.

AOA $< \Theta_y^2 >$ of the ordinary wave in the principle YOZ plane (location of an external magnetic field) increases from $8''$ up to $14''$ at $1 \le \chi \le 5$ and decreases to $6''$ in the interval $5 \le \chi \le 17$, while for the extraordinary wave decreases to $4''$. Contrary to the previous case, the wave structure function of the ordinary and extraordinary HF wave modes in the direction perpendicular to the principle plane not oscillates. Increasing anisotropy factor in the interval $\chi = 5 - 17$ the AOA $< \Theta_x^2 >$ increases: $12'' - 3'$. These statistical characteristics gives the information of plasma irregularities at high frequency radio waves propagation in the ionospheric F region.

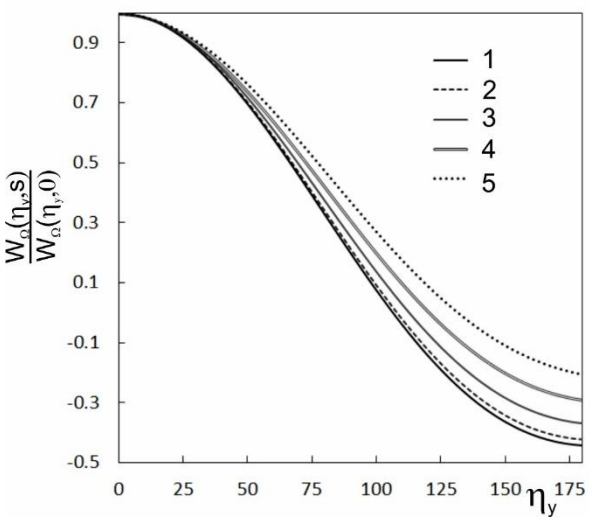

Fig. 4: Normalized correlation function of the phase fluctuations versus distance between observation points for different angle θ in isotropic case.

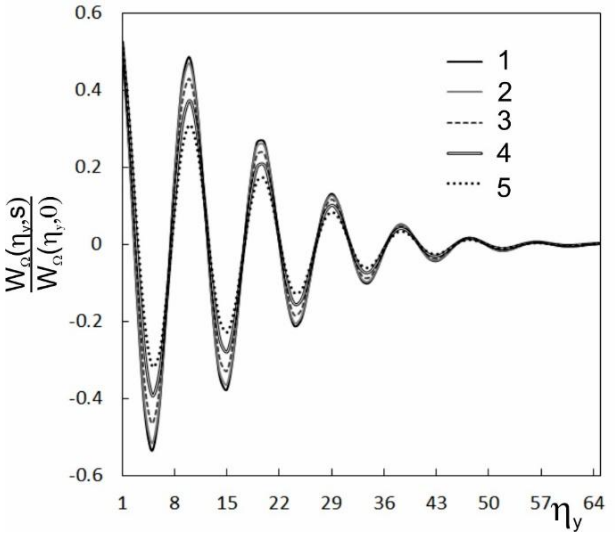

Fig. 5: Normalized correlation function of the phase fluctuations versus distance between observation points for different angle θ in anisotropic case.

Drift velocity of the ionospheric motions is in the interval $V_{dr} \approx 40-100$ m/sec [23]. Figures 4 and 5 illustrate the behavior of the normalized phase correlation function as a function of distance between observation points at different angle θ, $s=0.1$ and $\xi=150$ ($l_{\parallel} \approx 200$ m). Spatial anisotropy is caused by both: direction of a wind and elongated plasma irregularities. Numerical calculations show that in isotropic case ($\chi=1$, $\gamma_0=0^0$) of plasma irregularities SPS only broadens: at $\theta=10^0$ on 2% , at $\theta=20^0$ on 7%, at $\theta=30^0$ on 15%, at $\theta=40^0$ on 24% if the distance between observation points is 208 m. Movement of anisotropic irregularities substantially changes the shape of the SPS and the tail is appeared starting at $\eta_y=20$ m.

For relatively small irregularities diffraction effects are important. In such cases the interference between the direct ray from the transmitter and the scattered ray from the irregularity can result in a rapid fading of the received signal and hence scintillation. At investigation of the ionosphere by radiophysical methods parameters of inhomogeneous structure mainly are determined from the analyses of the diffraction pattern on the ground. Structure of the diffraction pattern substantially depends as on the ratio of the scale of irregularities and the Fresnel radius as well as on the phase fluctuations in the inhomogeneous slab. Observation of the scintillation of radio waves is connected with the investigation of the diffraction pattern on the ground level. Ionospheric scintillation depends on the 2D spectral correlation function of electron concentration fluctuations. The two asymptotic simplifications $\Upsilon << 1$ is associated with a significant filtering, non-fully developed diffraction pattern, whereas $\Upsilon >> 1$ is associated with a fully developed scintillation. Shaded area corresponds to a transition region between these two regions.

The relation between the phase fluctuations and scintillation indices is of interest. Substituting equation (16) into (11) scintillation level can be calculated. Figures 6 and 7 depicts the log-log plots of the normalized scintillation level $S_{4*} = S_4 / <\varphi_1^2>^{1/2}$ versus parameter $\Upsilon = (k_0 / k_f)^2$ for the anisotropic Gaussian spectral function at different parameters χ and γ_0; characteristic spatial scale of plasma irregularities along the geomagnetic lines of force is 120 m, normalized collision frequency is equal to $s=0.1$.

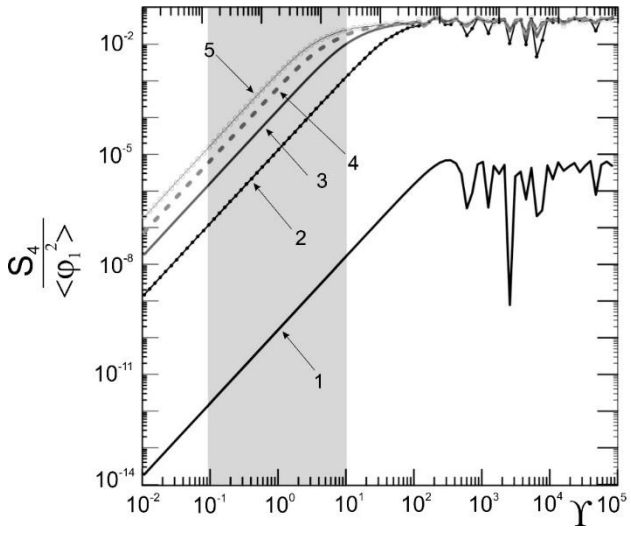

Fig. 6: Normalized scintillation level versus parameter Υ for different anisotropy coefficient χ and the angle γ_0. Designations are the same as on Fig. 2.

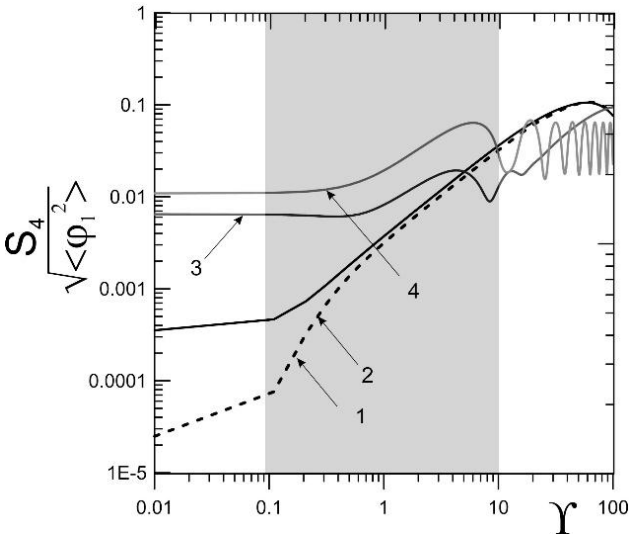

Fig. 7: Normalized scintillation spectrum versus parameter Υ for 3 MHz incident EM wave; $\xi=10$. Curve 1 corresponds to the isotropic case ($\chi=1$, $\gamma_0=0^0$), curve 2 ($\chi=5$, $\gamma_0=5^0$), curve 3 ($\chi=12$, $\gamma_0=15^0$).

On Figure 6 curve 1 corresponds to the isotropic case ($\chi=1$). In this case $S_{4*}=10^{-1}-10^{-3}$. Increasing anisotropy factor up to 20 (curve 5), scintillation level raises up to $S_{4*}=10^{-3}-10^{-2}$ on the altitude 250-400 km. Numerical calculations show that increasing frequency of an incident wave scintillation level substantially decreases in the ionospheric F region. For a sounding wave with frequency 40 MHz scintillation level less than for a probe wave having frequency 3 MHz. At the frequency 40 MHz weak scintillations occupy wide range of altitude if the diffraction parameter varies in the interval $10^2 \le \Upsilon \le 10^5$, corresponding to the altitudes 40-400 km. Analyses show that the collision between plasma particles has no substantial influence on the scintillation level in the high-latitude ionospheric F region.

Figure 7 illustrates scintillation level of scattered radiation of an incident wave 3 MHz ($k_0 = 6.28 \cdot 10^{-2}\ \mathrm{m}^{-1}$). Plasma parameters at an altitude of 300 km are: $u = 0.22$, $\mathrm{v} = 0.28$. Oscillations are observed since $\Upsilon = 25$ even at $\gamma_0 = 0^0$ (plasma irregularities are strongly elongated along geomagnetic lines of force) due to collision between plasma particles increasing parameter from $\chi = 25$. Oscillations are weakly damping up to $\Upsilon = 500$ and after they become stationary. The angle γ_0 has no influence on the oscillations amplitude up to $\chi \le 25$; starting at $\chi = 26$ oscillations become stationary from $\Upsilon = 18$ at arbitrary γ_0. In the case $\chi = 30$ and $\gamma_0 = 20^0$ oscillations become stationary starting from $\Upsilon = 38$. Small scintillation level corresponds to $S_{4*} < 0.5$ (the positive and negative intensity fluctuations with respect to the mean level) and big scintillation level $S_{4*} > 0.5$ is caused by the positive intensity fluctuations.

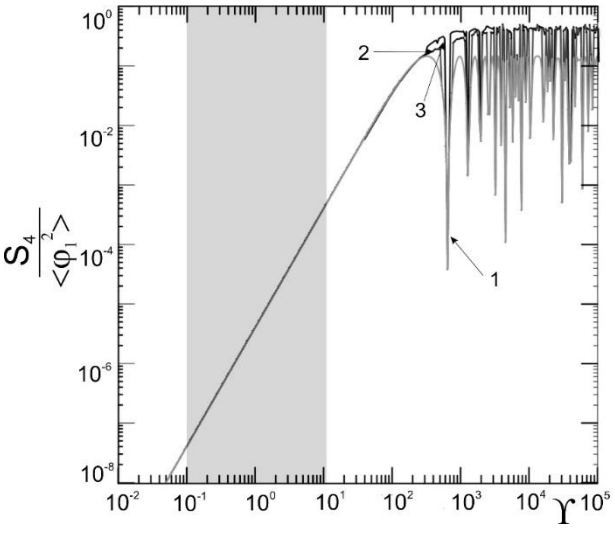

Fig. 8: Normalized scintillation level as a function of distance below an irregular plasma layer. Curve 1 correponds $k_0 L = 10^{-3}$, curve 2: $k_0 L = 10^{-2}$, curve 3: $k_0 L = 10^{-1}$. Characteristic spatial scale of plasma irregularities along the geomagnetic line of forces is 120 m.

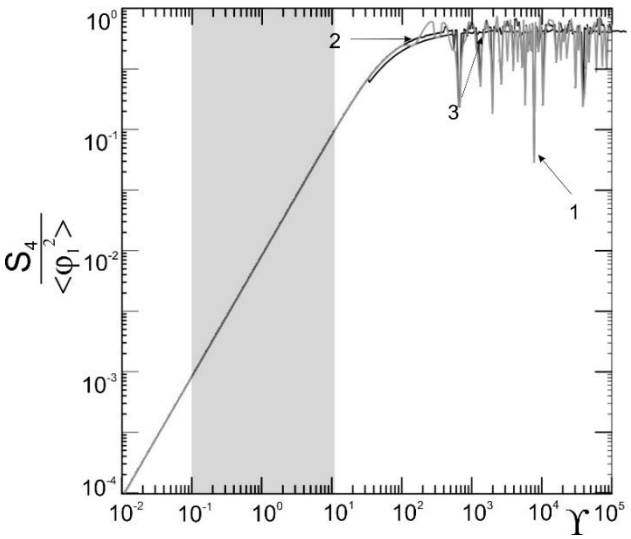

Fig. 9: Normalized scintillation level as a function of distance below an irregular plasma layer. Designations are the same as on Fig. 6; $l_{\|} = 240$ m.

Figures 8 and 9 illustrate the dependence of the function S_{4*} versus parameter Υ for different thickness of irregular plasma slab. Scintillations grow in proportion to the spread of a slab at small scale plasma irregularities aligned with the Earth's magnetic field lines at $l_{\|} = 120$ m. Big phase fluctuations of the radio wave in the magnetized turbulent plasma lead to the splashes of the diffraction pattern allowing to determine the heights of plasma irregularities causing this effect. Investigation of the intensity fluctuations of the receiving signals by spaced antennas show that splash effects mainly are caused by irregularities of the ionospheric F region locating on the altitudes 200-400 km. In some cases plasma irregularities are located on the height about 150 km. It should be also noted that at strong perturbations of the interference of recording satellite signals it is impossible to determine the location of plasma irregularities due to the absence of complete similarity between signals fluctuations in the spaced receiving antennas. Comparison of the scintillation level at the frequencies 3 MHz and 40 MHz show that the amplitude of scintillation decreases with increasing frequency of an incident wave. Scintillation level of scattered radio wave also depends on the spectrum of electron density irregularities.

In high latitude ionosphere the second order statistical moment of the phase fluctuations is:

$$< \varphi_1(\mathbf{r}) \varphi_1(\mathbf{r}+\boldsymbol{\rho}) > = -\frac{\pi}{2} (A + i\,B)\ k_0^2\, L \int_{-\infty}^{\infty} dk_x \int_{-\infty}^{\infty} dk_y\, V_n \left[k_x, k_y, \frac{1}{4k_0^2} (i\,\Lambda_3 - \Lambda_4) \right] \cdot \exp(-i\,k_x\,\rho_x - i\,k_y\,\rho_y), \quad (17)$$

where: $A = \tilde{Z}'^2 - s^2 \tilde{Z}''^2$, $B = 2 s \tilde{Z}' \tilde{Z}''$, $\Lambda_3 = -\frac{1}{4k_0^2} \left[2k_0 (\mathrm{P}''_j\, k_\perp - \Gamma''_j\, k_0) + \Gamma''_j\, k_y^2 \right] k_x + s (\mathrm{P}'_j\, \Gamma''_j - \mathrm{P}''_j\, \Gamma'_j)\, k_y\, k_x^2$,

$$\Lambda_4 = \frac{1}{4k_0^2}\left\{4k_0\,k_\perp\,k_y - \mathrm{P}''_j\,\Gamma''_j\,k_y\,k_x^2 + s\left[2k_0(\mathrm{P}'_j\,k_\perp - \Gamma'_j\,k_0) - \Gamma'_j\,k_y^2\right]\,k_x\right\}.$$

For the power-law spectrum (15) first and second approximations of the phase fluctuations are:

$$W_\varphi(\boldsymbol{\eta}) = \frac{\pi}{2}Q_0\,k_0\,L\,\frac{\chi^2}{\xi}\,(\tilde{Z}'^2 + s^2\,\tilde{Z}''^2)\int_{-\infty}^{\infty}dx\int_{-\infty}^{\infty}dy\;\frac{\exp(-i\,\eta_x\,x - i\,\eta_y\,y)}{\left[x^2+y^2+\chi^2\left(\frac{e_0}{4}+\frac{1}{\xi^2}\right)\right]^2}, \tag{18}$$

$$<\varphi_1^2> = \frac{\pi}{2}\,Q_0\,\frac{\xi^3}{\chi^2}\,(A - i\,B)\int_{-\infty}^{\infty}dx\int_{-\infty}^{\infty}dy\,(t_1\,x^2 + t_2\,y^2 \mp i\,t_3\,x\,y + 1)^{-\,p/2}, \tag{19}$$

$$2\,\mathrm{Re}<\varphi_2> = \mathrm{Re}\;\frac{\pi}{2}\,Q_0\,\frac{\xi^3}{\chi^2}\,(A + i\,B)\int_{-\infty}^{\infty}dx\int_{-\infty}^{\infty}dy\;\frac{1}{x^2+y^2}\left(-k_0\,L\left[(1+\varepsilon)\,x^2 + y^2\right] \pm \frac{1}{y\,(x^2+y^2)}\cdot\right.$$

$$\left.\left\{(1+\varepsilon)\,x(x^2+y^2) - (g_1\,x^2 + g_2) \mp i\,y\left[(1+\varepsilon)\,x^2 + y^2 + i\,(g_3\,x^2 + g_4)\right]\right\}\right)\cdot(t_1\,x^2 + t_2\,y^2 \mp i\,t_3\,x\,y + 1)^{-\,p/2}, \tag{20}$$

where: $Q_0 = \frac{\sigma_N^2}{\pi^{5/2}}\,\Gamma\left(\frac{p}{2}\right)\Gamma\left(\frac{5-p}{2}\right)\sin\left[\frac{(p-3)\pi}{2}\right]$, $t_1 = \frac{\xi^2}{\chi^2}\left[1 - \frac{1}{4}(1+\varepsilon)\,\mu^2\,\chi^2\right]$, $t_2 = \frac{\xi^2}{\chi^2}(1+\mu^2\chi^2)\,y^2$,

$t_3 = (1+\varepsilon)\,\xi^2\mu^2$, $\varepsilon = s^2\,\mathrm{P}''_2$, $\varphi = k_0\,L\,y^2$, $\mathrm{g}_1 = (x^2+y^2)(\cos\varphi - y\sin\varphi)$, $\mathrm{g}_3 = (x^2+y^2)(\sin\varphi + y\cos\varphi)$,

$g_2 = \varepsilon\left[(3\cos\varphi \mp 2y\sin\varphi)\,x^2 + y^2\cos\varphi\right]$, $g_4 = \varepsilon\left[(3\sin\varphi \pm 2y\cos\varphi)\,x^2 + y^2\sin\varphi\right]$.

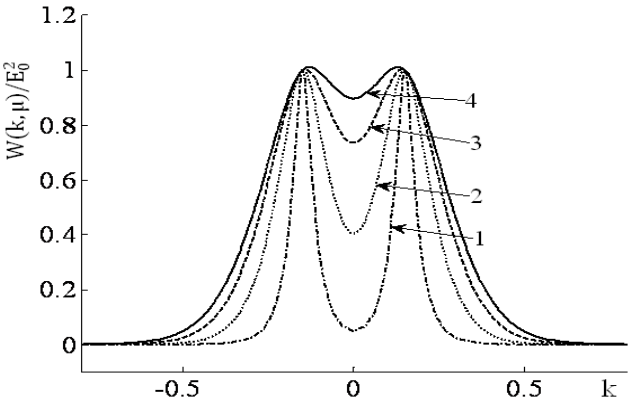

Fig. 10: The normalized SPS of a scattered field in the ionospheric F-region for different anisotropy factor of plasma irregularities. Curve 1 corresponds to the $\chi = 1$, curve 2: $\chi = 2$, curve 3: $\chi = 3$, curve 4: $\chi = 4$.

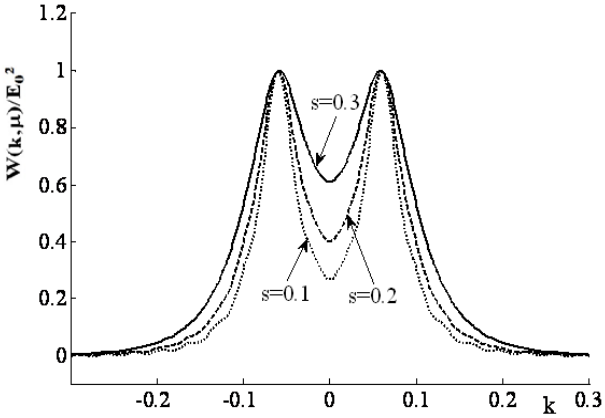

Fig. 11: The normalized SPS of scattered electromagnetic waves for different collision frequencies between plasma particles. Parameter s varies in the interval 0.1-0.3.

r the

characteristic spatial scale of irregularities $l_\parallel = 120$ km, $\beta = 10$, $s = 0.01$. The curves of the SPS have two symmetrical maximums. In the isotropic case ($\chi = 1$) maximums are at: $k = \pm 0.15$ and minimum is at $k = 0.005$; for $\chi = 2$ maximums are at: $k = \pm 0.149$ and minimum at: $k = 0.04$; for $\chi = 3$ maximums are at: $k = \pm 0.143$ and minimum at: $k = 0.07$; for $\chi = 4$ maximums are at: $k = \pm 0.133$ and minimum at: 0.09. Increasing parameter of anisotropy χ dip of a gap of the SPS decreases two times. Decreasing both anisotropy factor χ and the collision frequency s the depth of a curve increases.

CONCLUSION

Second order statistical moments of scattered radio wave in the turbulent collision magnetized plasma are investigated for both anisotropic Gaussian and power-low correlation functions of electron density fluctuations using the modify smooth perturbation method taking into account polarization coefficients of the ordinary and extraordinary HF wave modes and the

diffraction effects. Analytical and numerical calculations are carried out for both small and large scale plasma irregularities. Correlation function of the phase fluctuations fast decreases for both wave modes, while oscillations are observed at big anisotropy factors of elongated irregularities. The behavior of the phase structure function of the ordinary and extraordinary waves is different in the principle (location of an external magnetic field) plane while the same in the perpendicular plane. Anisotropy, diffraction effects and collision between plasma particles have substantial influence on the phase structure function of the extraordinary wave in the principle plane. This statistical characteristic allows to calculate AOAs. Varing anisotropy factor the AOA in the principle plane less than in the perpendicular one. They are determined by geometry of ionospheric plasma irregularities which are necessary for the solution of the inverse problems.

Scintillation effects are investigated numerically using anisotropic Gaussian correlation function at field-aligned and field-perpendicular small scale anisotropic irregularities of electron concentration fluctuations. It was shown that scintillation level of scattered radio wave depends on the spectrum of electron density irregularities and substantially decreases increasing frequency of an incident wave from 3 MHz up to 40 MHz scintillation level. Splashes caused by the strong phase fluctuations are revealed in the normalized scintillation level at 40 MHz frequency. The study of scintillations enable to obtain some information about the nature of the irregularities. Measuring the intensity scintillation index and the variance of phase it might be able to deduce parameters of the ionospheric irregularities producing scintillation. Double-humped shape has revealed in the SPS for large scale plasma irregularities. Decreasing both anisotropy factor and collision frequency the depth of a curve increases at fixed collision frequency.

The obtain results might be useful for remote sensing purposes and for communication-channel modeling.

ACKNOWLEDGMENTS

This work has been supported by the International Science and Technology Center (ISTC) under Grant # G-2126 and Shota Rustaveli National Science Foundation under Grant # FR/3/9-190/14.

REFERENCES

1. Ishimaru, A. 1997. Wave Propagation and Scattering in Random Media, Vol. 2, Multiple Scattering, Turbulence, Rough Surfaces and Remote Sensing, IEEE Press, Piscataway, New Jersey, USA.
2. Frolov, V.L., N.V. Bakhmet'eva, V.V. Belikovich, G.G. Vetrogradov, V.G. Vatrogradov, G.P. Komrakov, D.S. Kotik, N.A. Mityakov, S.V. Polyakov, V.O. Rapoport, E.N. Sergeev, E.D. Tereshchenko, A.V. Tolmacheva, V.P. Uryadov, and B.Z. Khudukon. 2007, Modification of the earth's ionosphere by high-power high-frequency radio waves, Phys. Usp., vol. 50, 315-325.
3. Xu, Z.-W., J. Wu, and Wu, Z.-S. 2004. A survey of ionospheric effects on space-based radar, Waves in Random media, vol. 14, S189-S273.
4. Wernik, A.W., Secan, J.A., and Fremouw, E.J. 2003. Ionospheric irregularities and scintillation. Advances Space Research., vol. 31, # 4, 971–981.
5. Wu, Z.-S., Wei, H.-Y., Yang, R.-K., and Guo, L.-X. 2008. Study of scintillation considering inner and outer-scales for laser beam propagation on the slant path through the atmospheric turbulence, PIER vol. 80, 277-293.
6. Gershman, B.N., Erukhimov, L.M., and Yashin, Yu.Ya. 1984. Wave phenomena in the Ionosphere and Space Plasma, Moscow, Nauka.
7. Jandieri, G.V., Ishimaru, A., Jandieri, V.G., Khantadze, A.G. and Diasamidze, Zh.M. 2007. Model computations of angular power spectra for anisotropic absorptive turbulent magnetized plasma. PIER vol. 70, 307-328.
8. Jandieri, G.V., Ishimaru, A., Rawat B.S. and Tugushi, N.K. 2015. Peculiarities of the spatial power spectrum of scattered electromagnetic waves in the turbulent collision magnetized plasma. PIER, vol. 152, 137-149.
9. Jandieri, G.V., Diasamidze, Zh.M., and Diasamidze, M.R.. 2013. Scintillation spectra of scattered electromagnetic waves in turbulent magnetized plasma. Journal of Basic and Applied Physics, vol. 2, 224-234.
10. Jandieri, G.V., Ishimaru, A., Mchedlishvili, N.F., and Takidze, I.G. 2012. Spatial power spectrum of multiple scattered ordinary and extraordinary waves in magnetized plasma with electron density fluctuations. PIER M, vol. 25, 87-100.
11. Jandieri, G.V. 2016. „Double-Humped Effect" in the turbulent collision magnetized plasma. PIER M, vol. 48, 95-102.
12. Ginzburg, V.L. 1961. Propagation of Electromagnetic Waves in Plasma, Gordon and Beach, New York.
13. Jandieri G.V., and Ishimaru, A. 2013. Some peculiarities of the spatial power spectrum of scattered electromagnetic waves in randomly inhomogeneous magnetized plasma with electron density and external magnetic field fluctuations, PIER B, vol. 50, 77-95.
14. Tatarskii V.I.. 1961. Wave Propagation in a Turbulent Medium, McGraw-Hill, New York.

15. Jandieri, G.V., Zhukova, N.N., Takidze, I.G., and Jandieri, I.V. 2012. Statistical characteristics of scattered radiation in medium with spatial-temporal fluctuations of electron density and external magnetic field. Journal of Electromagnetic Analysis and Application, vol. 4, 243-251.

16. Rufenach C. L. 1972. Power-law wavenumber spectrum deduced from ionospheric scintillation observations. Journal of Geophysical Research, vol. 77, 4761-4772.

17. Jandieri G.V., Gavrilenko, V.G., and Aistov, A.V. 2000. Some peculiarities of wave multiple scattering in a statistically anisotropic medium, Waves Random Media, vol. 10, 435-445.

18. Jandieri G.V., Gavrilenko, V. G., Ishimaru A., and Jandieri V.G. 2008. Peculiarities of spatial spectrum of scattered electromagnetic waves in anisotropic inhomogeneous medium. PIER B, vol. 7, 191–208.

19. Rytov, S.M., Kravtsov, Yu.A. and Tatarskii, V.I. 1989. Principles of Statistical Radiophysics. vol.4. Waves Propagation Through Random Media. Berlin, New York, Springer.

20. Prakash, S.S., Pal, S., and Chandra, H. 1991. In-situ studies of equatorial spread F over SHAR-steep gradients in the bottomside F-region and transitional wavelength results. J. Atmos. Terr. Phys., vol. 53, 977-986.

21. Raizada, S., and Sinha, H.S.S. 2000. Some new features of electron density irregularities over SHAR during strong spread F. Ann. Geophysicae, vol. 18, 141-151.

22. Gailit, T.A., Gusev, V.D., Erukhimov, L.M. and Shpiro, P.I. 1983. On spectrum of phase fluctuations at ionospheric remote sensing. Radiophysics, vol. 26, 795-800 (in Russian).

23. Bakhmet'eva, N.V., Bubukina, V.N., Ignat'ev, Yu.A., Bochkarev, G.S., Eremenko, V.A., Kol'sov, V.V., Krasheninnikov, I.V. and Cherkashin, Yu.N. 1997. Investigation by backscatter radar irregularities produced in ionospheric plasma heating experiments. 1997. Journal of Atmospheric and Terrestrial Physics, vol. 59, 2257-2263.